The low-lying excited states of neutral polyacenes and their radical cations: a quantum chemical study employing the algebraic diagrammatic construction scheme of second order

Stefan Knippenberg, Jan-Hendrik Starcke, Michael Wormit, Andreas Dreuw

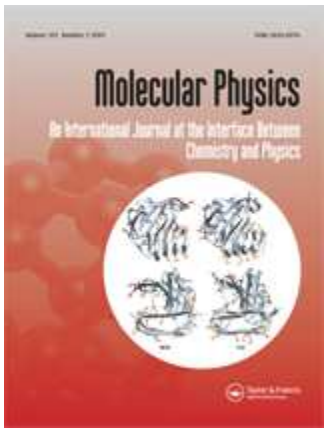

The low-lying excited states of neutral polyacenes and their radical cations: a quantum chemical study employing the algebraic diagrammatic construction scheme of second order

Journal:	*Molecular Physics*
Manuscript ID:	TMPH-2010-0370
Manuscript Type:	Special Issue Paper - MQM 2010
Date Submitted by the Author:	16-Sep-2010
Complete List of Authors:	Knippenberg, Stefan; University of Frankfurt, Institute of Physical and Theoretical Chemistry Starcke, Jan-Hendrik; University of Frankfurt, Institute of Physical and Theoretical Chemistry Wormit, Michael; University of Frankfurt, Institute of Physical and Theoretical Chemistry Dreuw, Andreas; University of Frankfurt, Institute of Physical and Theoretical Chemistry
Keywords:	electron propagator, algebraic diagrammatic construction, excited states, polyacenes, radical cations
Note: The following files were submitted by the author for peer review, but cannot be converted to PDF. You must view these files (e.g. movies) online.	
Submit.zip	

Molecular Physics
Vol. 00, No. 00, Month 2010, 1–18

RESEARCH ARTICLE

The low-lying excited states of neutral polyacenes and their radical cations: a quantum chemical study employing the algebraic diagrammatic construction scheme of second order

Stefan Knippenberg, Jan Hendrik Starcke, Michael Wormit and Andreas Dreuw*

Institut für Physikalische und Theoretische Chemie, Goethe-Universität Frankfurt, Max von Laue-Str. 7, 60438 Frankfurt, Germany

(*Received 00 Month 200x; final version received 00 Month 200x*)

The vertical excited electronic states of linearly fused neutral polyacenes and their radical cations have been investigated using the algebraic diagrammatic construction scheme of second order (ADC(2)). While strict ADC(2) (ADC(2)-s) correctly reproduces trends for mainly singly excited states, in extended ADC(2) (ADC(2)-x) the description of doubly excited states is critically improved. It is shown that a combined application of strict and extended ADC(2) nicely reveals the importance of doubly excited configurations in the description of the excited state spectrum of the neutral polyacenes. In contrast to general expectation, our calculations of the lowest excited states of the radical cations of the polyacenes employing unrestricted ADC(2)-s and ADC(2)-x identified one B_{1g} electronic transition whose excitation energy increases with increasing molecular size. Thorough analysis of this electronic state and the involved molecular orbitals relates this unusual phenomenon to an increasing energy gap between the doubly occupied molecular orbital, out of which an electron is excited, and the singly occupied orbital, into which it is excited.

Keywords: electron propagator, algebraic diagrammatic construction, excited states, polyacenes, radical cations

1. Introduction

The development of efficient quantum chemical methods for the accurate calculation of excited state properties of large molecular systems is one of the greatest challenges of modern theoretical chemistry [1, 2]. Today, several excited state methods are already available for the investigation of large molecules, among which time-dependent density functional theory (TDDFT) [3–5] is by far the most widely used. Complete active-space self-consistent field (CASSCF) methods [6, 7], symmetry-adapted cluster configuration interaction (SAC-CI) [8] and also approximate linear-response coupled-cluster theory of second order (RI-CC2) [9–12] are powerful wavefunction-based approaches. Nevertheless, all existing methods possess individual weaknesses and drawbacks [1, 2]. The success of the available methods is manifested by ample excellent applications in the fields of photochemistry and photobiology [13–24].

Even more than for closed-shell molecules, theoretical methods are urgently needed to reliably provide information about excited states of open-shell molecules, since neutral and charged radicals are of crucial importance in a broad range of chemical and biological processes. Unrestricted formulations and implementations

*Corresponding author. Email: andreas.dreuw@theochem.uni-frankfurt.de

ISSN: 00268976 print/ISSN 13623028 online

DOI: 10.1080/0026897YYxxxxxxxx
http://www.informaworld.com

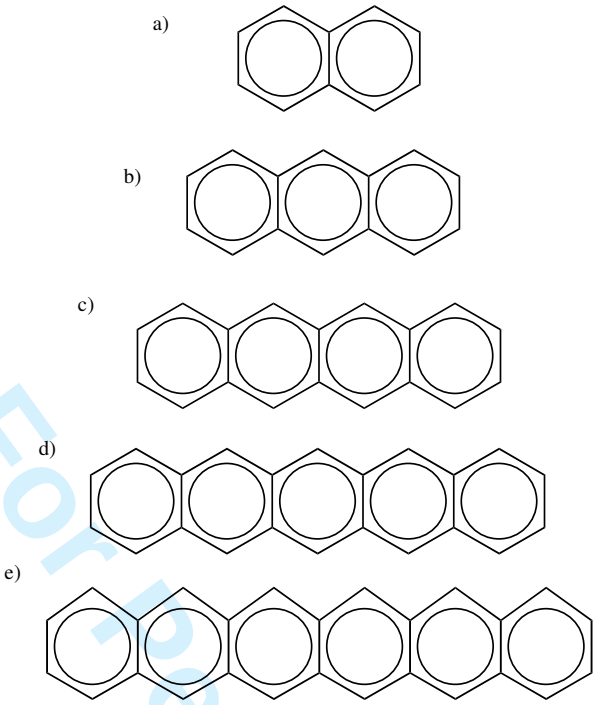

Figure 1. Molecular structure of the linearly fused polyacenes from a) naphthalene to b) anthracene, c) tetracence, d) pentacene and e) hexacene.

of coupled cluster (CC) methods like equation-of-motion CC (EOM-CC)[25, 26] and linear response CC (LR-CC) [27–29] provide good results for excited states of smaller open-shell molecules, while approximate CC methods like CC2 [10, 12] and CASSCF theories [30–32] are available for medium-sized radicals, too. Of course, TDDFT can also be employed to compute electronic spectra of radicals. However, here one certainly faces all problems known from closed-shell systems [5].

An elegant, however, until today mostly overseen method for the calculation of excited states is the algebraic diagrammatic construction (ADC) scheme of the polarization propagator [33–37], originally derived in the realm of Green's function theory [38, 39]. The recent development of efficient computer codes for ADC is a prerequisite for its routine application to molecular systems of chemical and biophysical interest [40–43]. Although the ADC scheme is general and can be expanded to arbitrarily high-orders in perturbation theory, only second order ADC (ADC(2)) is currently computationally efficient enough to be applicable to large and medium-sized molecules on present-day computers. Recently, the ADC(2)-x scheme has been extended to an unrestricted spin-orbital formalism allowing for the calculation of excited states of open-shell radicals [42, 43]. For energetically low-lying states of medium-sized open-shell doublet radicals, the UADC(2)-x scheme turned out to yield excitation energies with an overall accuracy of about 0.3 eV [42].

In this work, ADC and UADC schemes are employed to investigate the vertical excited states of neutral, linearly fused polyacenes (PAC) and their radical cations. In figure 1, the series from naphthalene with two fused rings up to hexacene with six rings is displayed. Polyacenes belong to the class of polycyclic aromatic hydrocarbons (PAHs) which form a large group of conjugated π-electron systems of fundamental importance in many research areas of chemistry as well as in astro-

physics and materials science [44–46].

Polyacenes pose a challenge to quantum chemistry, because the extended π electron conjugation leads to long-range electron correlations, which must be taken into account for a meaningful description of the electronic structure and, thus, of many physical and chemical properties (see for example [47–53]). Therefore, the linear PACs and their radical cations represent excellent test sets to explore the applicability and the limits of the restricted and unrestricted ADC(2) methods.

In this work, we focus on the energetically low-lying excited electronic states of the neutral polyacenes naphthalene up to hexacene and their radical cations in the near UV and visible range of the optical spectrum. In particular, the influence of doubly excited states in that energy regime lies at the heart of our study, which will be discussed in detail below. On one hand the accuracy of the ADC(2) schemes and its applicability to these highly correlated class of conjugated systems shall be investigated. On the other hand, some more light is to be shed on the excited states and their properties, in particular on the ones of the radical cations, which have only been scarcely studied theoretically so far.

The paper is organized as follows. For the paper to be self-contained and since ADC is a rather uncommon approach, we briefly review the derivation of the ADC(2) schemes in Section 2, where also a brief comparison to other excited states methods is made. After presenting the computational details, first the low-lying excited states of neutral polyacenes will be studied and compared to existing literature values in section 4. Then, we will focus onto the excited states of the corresponding radical cations (Section 5) The paper concludes with a brief summary of the major results and an outlook (Section 6).

2. Theory

Algebraic expressions of the ADC scheme for excited states have first been derived for closed-shell molecules employing diagrammatic perturbation theory of the polarization propagator using the typical Møller-Plesset partition of the Hamilton operator [33–35, 54]. From that point of view, the choice of the otherwise unusual name becomes obvious. However, in addition, the ADC equations can be derived in an elegant way employing the intermediate state representation (ISR) [37], which will be presented in the following in a little bit more detail. Besides an elegant derivation, the ISR also provides access to the wavefunctions of the excited states and thus to the computation of excited state properties.

The starting point of the derivation of the ADC scheme via ISR is the exact N-electron ground state wavefunction $|\Psi_0^N\rangle$, to which physical excitation operators are applied to generate a "correlated" set of excited state wavefunctions $|\Psi_J^0\rangle$

$$|\Psi_J^0\rangle = \hat{C}_J|\Psi_0^N\rangle, \tag{1}$$

with

$$\{\hat{C}_J\} = \{c_a^\dagger c_k; c_a^\dagger c_k c_b^\dagger c_l, a < b, k < l; \dots\}, \tag{2}$$

where the operators $c_p^\dagger(c_p)$ of second quantization are associated with one-particle states $|\phi_p\rangle$ of the Hartree-Fock ground state $|\Phi_0^N\rangle$. As usual, the subscripts $a, b, c, \dots, i, j, k, \dots, p, q, r, \cdots$ label unoccupied (virtual), occupied and general orbitals, respectively. The excitation operators $\hat{C}_J$ naturally decompose into classes depending on the number of electrons that are excited.

Although these "correlated" excited states form a complete set of N-electron states provided that $\langle\Psi_0^N|\Phi_0^N\rangle \neq 0$ [55, 56], they are not orthonormal. However, it is always possible to construct an orthonormal basis by successive Gram-Schmidt orthogonalization of the excitation classes starting from the exact ground state, the singly excited states, doubly excited states, etc. eventually leading to the so-called intermediate states (IS) $|\tilde{\Psi}_J\rangle$ [57, 58]. Finally, it is obvious that the exact excited states $|\Psi_n\rangle$ can be represented in this IS basis via

$$|\Psi_n\rangle = \sum_J X_{nJ}|\tilde{\Psi}_J\rangle. \tag{3}$$

To arrive at algebraic expressions to compute excitation energies, one represents the shifted Hamiltonian $\hat{H} - E_0$ in the IS basis to obtain

$$\langle\tilde{\Psi}_I|\hat{H} - E_0^N|\tilde{\Psi}_J\rangle = \langle\Psi_0^N|\tilde{C}_I^\dagger[\hat{H}, \tilde{C}_J]|\Psi_0^N\rangle = M_{IJ}. \tag{4}$$

Diagonalization of the hermitian ADC matrix $\mathbf{M}$, i.e. solution of the corresponding ISR secular equation,

$$\mathbf{MX} = \mathbf{X\Omega}, \qquad \mathbf{X}^\dagger\mathbf{X} = 1, \tag{5}$$

yields as eigenvalues the excitation energies,

$$\Omega_n = E_n - E_0, \tag{6}$$

and as eigenvectors the coefficients of the exact excited states in the IS expansion (eq. 3). In general, the transition dipole moments

$$T_n = <\Psi_n|\hat{\mu}|\Psi_0>, \tag{7}$$

where $\hat{\mu}$ is the typical dipole operator, are given by

$$T_n = \mathbf{X}_\mathbf{n}^\dagger\mathbf{F}(\mu) \tag{8}$$

as the scalar products of the eigenvectors $\mathbf{X}_n$ with the so-called effective transition moments $\mathbf{F}(\mu)$. The corresponding oscillator strength is obtained according to the standard expression

$$f_n = \frac{2}{3}\Omega_n < T_n >^2 . \tag{9}$$

Note that the derivation started from the *exact* correlated ground state wavefunction yielding a full-ADC scheme providing *exact* excitation energies and transition moments. However, the exact ground state is of course not known, and thus one has to resort to a suitable approximation as starting point and to derive the corresponding ISR matrix elements. In fact, the level of approximation of the ground state wave function determines the order of the ADC scheme. For example, when an MP2 ground state is chosen, the corresponding ISR derivation yields ADC(2), MP3 results in ADC(3), etc. The algebraic expressions of the matrix elements M_{IJ} (eq. (4)) are typical perturbation theoretical expressions, which have been derived in detail for ADC(2) and ADC(3) in Refs. [34–36]. Since the ADC(n) excitation energies are computed with respect to the corresponding MPn ground state, ADC(2),

for instance, should only be applied to molecular systems whose ground state is well described by a single determinant such that MP2 is a reasonable approximation.

The extension of the ISR formalism to a spin-orbital basis is straightforward and enables the derivation of unrestricted ADC schemes [42]. These UADC schemes can be employed to compute excited states of open-shell radicals. The major changes in the derivation occur in the choice of the excitation operators in equation (2), where now attention has to be paid that successive annihilation and creation operators act on spin-orbitals with the same spin, thereby excluding so-called spin-flip excitations in which the spin state of the excited electron is changed. Furthermore, UMP2 must be chosen as ground state reference to eventually derive UADC(2).

A *strict* and an *extended* variant of ADC(2) have been developed [34], and are further referred to as ADC(2)-s and ADC(2)-x, respectively. While in the former scheme couplings between doubly excited configurations are not contained in the $2p2h/2p2h$ block of the ADC matrix, i.e. the $2p2h/2p2h$–block of $\mathbf{M}$ is diagonal, they are included to first order in an *ad hoc* fashion in ADC(2)-x. Originally these first-order coupling terms stem from the higher-order ADC(3) scheme. Nevertheless, their inclusion leads to an overall improved treatment of excited states with double excitation character in the ADC(2)-x scheme. Typically, excited states with significant double excitation character are energetically too high in ADC(2)-s, and their energy decreases substantially relative to states with mostly single excitation character when ADC(2)-x is used. Thus, both schemes can be used in comparison to detect appearance and importance of low-lying doubly excited states, as has been demonstrated previously for the $2A_g^-$ state of linear polyenes [41].

From a numerical point of view, ADC combines perturbation theory with configuration interaction (CI). It is size-consistent and, in addition, the ADC matrix $\mathbf{M}$ is hermitian. Moreover, ADC is more compact than CI or CC. Compactness is generally defined as the size of the configuration space required to describe ground and singly excited states consistently through a particular order of perturbation theory. While CI methods generally require the full configuration space, i.e. for a consistent treatment of these primary states to say nth order of perturbation theory one needs all n-tuply excited configurations. When the order of perturbation theory is even, say $2m$, both ADC and CC are identically compact and require a configuration space of $m+1$. For odd orders of perturbation theory, $2m+1$, ADC is slightly more compact with a configuration space size of also $m+1$ compared to $m+2$ for the CC methods. For a detailed comparison of ADC, CC and CI the reader is referred to [54, 59, 60].

3. Computational Details

The geometrical parameters of the neutral polyacenes and their radical cations have been optimized employing second order Møller-Plesset perturbation theory (MP2) together with Pople's 6-31G* basis set. For the open-shell radical cations an unrestricted Hartree-Fock reference (UHF) has been employed throughout all reported calculations. The vertical excited states have been calculated using the strict and extended ADC scheme of second order, ADC(2)-s and ADC(2)-x, respectively, which have been implemented into a development version of the QCHEM-3.2 quantum chemistry program package [61]. For comparison, the B_{2u} and B_{3u} excited states of the neutral compounds have been computed also with the equation-of-motion coupled cluster singles and doubles (EOM-CCSD) method [29, 62]. Throughout the calculations the core electrons have been frozen, and the D_{2h} symmetry point group has been exploited. The vertical excited states of the polyacene radical cations have also been calculated using unrestricted TDDFT in combina-

tion with the hybrid Becke three-parameter Lee-Yang-Parr (B3LYP) xc-functional and the 6-31G* basis set [3–5].

4. Excited State Properties of Neutral Polyacenes

Neutral linearly fused polyacenes possess D_{2h} symmetry, and a closed-shell A_{1g} electronic ground state. They are well-known to possess two prominent excited states in the low energy region dominating the experimental absorption spectrum: a short-axis polarized, so-called L_a (B_{2u}) state and a long-axis polarized L_b (B_{3u}) state. The existence of other dark excited states in this energy region has been indicated by early two-photon absorption spectra of naphthalene, in which an excited state with *gerade* symmetry has been observed around 5.5 eV [63–65]. More than thirty years ago, Tavan and Schulten computed the excited states of linearly fused polyacenes from naphthalene up to pentacene using a configuration interaction doubles (D-CI) approach based on the semi-empirical Pariser-Parr-Pople (PPP) Hamiltonian [66]. Already then, they noticed the importance of double excitations for a reliable treatment of the low-lying excited states of these molecules. "New" doubly excited states with *gerade*-symmetry were observed, and indeed A_g was found to drop energetically below the optically allowed B_{3u} state when the number of fused benzene rings reaches five, i.e. pentacene. In addition, the B_{2u} (L_a) and B_{3u} (L_b) states were found to change order from naphthalene to tetracene, the former becoming lower in energy than the latter. In a recent study, the excited electronic states of these neutral polyacenes have been re-investigated by Marian and Gilka using a semi-empirical DFT/MRCI approach [67]. Their results agree largely with the early calculations of Tavan and Schulten. The low-lying doubly excited A_g and B_{1g} states have been confirmed, and the A_g state has been shown to become even the lowest excited state from hexacene on.

Recently, Parac and Grimme pointed out that TDDFT yields substantial errors even in the description of the B_{2u} (L_a) state while its counterpart B_{3u} (L_b) is described reasonably well [68, 69]. CC2, on the other hand provides a balanced description of these two states in good agreement with the experiment [68]. Since both the CC2 method and TDDFT are not capable of describing doubly excited states accurately, one can exclude these TDDFT problems to arise from double excitation character, as it is for instance the case for the 2 A_g^- state of linear polyenes [41] or as it would be for the A_g and B_{1g} states of the polyacenes as we will see later.

All reported studies including also excited states of the polyacenes with *gerade* symmetry rely on multi-reference treatments based on some semi-empirical model Hamiltonian. Note that also the DFT/MRCI approach used by Marian and Gilka and devised by Grimme also contains semi-empirical parameters to screen the Coulomb integrals [16]. Here, on the other hand, *ab initio* single-reference ADC(2) as well as EOM-CCSD approaches have been used to calculate the vertical excited states of the neutral linearly fused polyacenes from naphthalene up to hexacene, and the obtained results for the lowest 1^1B_{3u} (L_b), 1^1B_{2u} (L_a), 2^1A_g and 1^1B_{1g} states are compiled in Table 1.

For naphthalene the 1^1B_{3u} (L_b) state corresponds to the lowest excited S_1 state at all employed levels of theory supported by the known experimental excitation energy. This state is well described as a single excitation, and can be represented as linear combination of HOMO-1→LUMO and HOMO→LUMO+1 excited determinants. While ADC(2)-s, EOM-CCSD, TDDFT/B3LYP and CC2 yield very similar values, they all overestimate the vertical excitation energy by about 0.4-0.5 eV, and only DFT/MRCI gives an excitation energy of 4.15 eV in remarkable agreement

Table 1. Computed vertical excitation energies (eV) and oscillator strengths (in parenthesis) of the four lowest excited states of the neutral polyacenes naphthalene (2) to hexacene (6) at ADC(2)-s, ADC(2)-x and EOM-CCSD level of theory compared with literature data at DFT/MRCI, TDDFT and CC2 level and experimental values.

n	ADC(2)-s	ADC(2)-x	EOM-CCSD	DFT/MRCI[a]	TDDFT/B3LYP[b]	CC2[b]	Expt.[c]
1^1B_{3u} (L_b)							
2	4.57 (0.000)	3.51 (0.000)	4.47	4.15	4.47	4.46	4.13
3	4.00 (0.001)	3.01 (0.001)	3.94	3.59	3.87	3.89	3.64
4	3.61 (0.002)	2.67 (0.002)	3.58	3.22	3.47	3.52	3.39
5	3.36 (0.000)	2.42 (0.000)		2.99	3.21	3.27	3.12
6	3.18 (0.000)	2.28 (0.000)		2.76	3.02	3.09	2.87
1^1B_{2u} (L_a)							
2	5.09 (0.104)	4.47 (0.098)	5.37	4.66	4.38	4.88	4.66
3	3.87 (0.109)	3.27 (0.092)	4.22	3.51	3.21	3.69	3.60
4	3.04 (0.102)	2.46 (0.081)	3.44	2.74	2.43	2.90	2.88
5	2.46 (0.000)	1.90 (0.000)		2.22	1.89	2.35	2.37
6	2.05 (0.000)	1.49 (0.000)		1.85	1.49	1.95	2.01
2^1A_g							
2	6.44 (0.000)	5.04 (0.000)	6.39	5.73			
3	5.78 (0.000)	3.79 (0.000)	5.76	4.60			
4	5.08 (0.000)	2.55 (0.000)	5.11	3.37			
5	4.53 (0.000)	1.57 (0.000)		2.52			
6	4.12 (0.000)	0.77 (0.000)		1.86			
1^1B_{1g}							
2	6.54 (0.000)	5.26 (0.000)	6.85	5.63			
3	5.38 (0.000)	4.20 (0.000)	5.75	4.46			
4	4.41 (0.000)	3.35 (0.000)	4.82	3.62			
5	3.68 (0.000)	2.70 (0.000)		3.00			
6	3.12 (0.000)	2.21 (0.000)		2.44			

[a]Taken from Ref. [67], who used DFT/B3LYP/TZVP optimized ground state geometries.

[b]Taken from Ref. [68]

[c]Taken from Ref. [47] and corrected for solvent and relaxation effects according to Ref. [68]

with the experimental value of 4.13 eV. When going from ADC(2)-s to ADC(2)-x, i.e. improving the description of doubly excited states to first order, its excitation energy drops by 1 eV from 4.57 to 3.51 eV, despite its mainly single excitation character. As a consequence, ADC(2)-x, underestimates the vertical excitation energy by 0.6 eV. Not discussing the vertical excitation energies of the 1^1B_{3u} state of all larger linear polyacenes individually, which are listed in Table 1, an overall identical trend is observed also for the larger polyacenes.

The 1^1B_{2u} (L_a) is the second lowest excited S_2 state of naphthalene, exhibiting an experimental excitation energy of 4.66 eV. Also this state corresponds to a singly excited state almost exclusively represented as HOMO→LUMO excitation. ADC(2)-s, EOM-CCSD and CC2 tend to overestimate the vertical excitation energy by 0.7-0.2 eV, while TDDFT/B3LYP underestimates it by 0.3 eV. DFT/MRCI is the only method which agrees excellently with the experimental value. Comparison of the computed ADC(2)-s and ADC(2)-x values of this state of 5.09 and 4.47 reveals again a large drop in excitation energy, although not as pronounced as for the 1^1B_{3u} state above. In the case of the 1^1B_{2u} state, the accuracy of the DFT/MRCI method degrades slightly when going to larger polyacenes, which may be related to size-consistency problems. For ADC(2)-s, EOM-CCSD, and CC2, the relative error in excitation energies remains essentially the same or

improves slightly with increasing number of fused benzene rings. Astonishingly, TDDFT/B3LYP and ADC(2)-x show a very similar behavior, despite the very different nature of the methods, and give essentially identically poor values for the larger polyacenes. Both methods underestimate the excitation energy of the 1^1B_{2u} state of hexacene by 0.5 eV. Comparison of the computed and experimental values of the 1^1B_{3u} (L_b) and 1^1B_{2u} (L_a) states shows that the 1^1B_{2u} state is essentially degenerate with 1^1B_{3u} for anthracene and becomes the lowest excited state for the larger polyacenes. This trend is correctly reproduced by all methods described above, only TDDFT/B3LYP falsely designates the 1^1B_{2u} excited state as the lowest one already for naphthalene.

The lowest excited state with *gerade* symmetry and in total the third lowest excited S_3 state of naphthalene is the 2^1A_g state at ADC(2)-s, ADC(2)-x and EOM-CCSD level (Table 1) exhibiting vertical excitation energies of 6.44 eV, 5.04 eV and 6.39 eV at these levels of theory, respectively. At DFT/MRCI level, the vertical excitation energy of the 2^1A_g state is 5.73 eV. However, the difference can easily be due to the different ground state geometries employed within the former and the latter calculations. Nevertheless, the huge drop in excitation energy of 1.4 eV of the 2^1A_g state in the transition from ADC(2)-s to ADC(2)-x reveals the importance of doubly excited configurations for the proper description of this state. Indeed, the 2^1A_g is best described as a $HOMO^2 \rightarrow LUMO^2$ double excitation. Still, ADC(2)-x clearly underestimates the vertical excitation energy by about 0.7 eV compared to the DFT/MRCI value. In view of the good accuracy of the DFT/MRCI approach in the description of the 1^1B_{3u} and 1^1B_{2u} states above, the DFT/MRCI values are certainly the most reliable ones also for the 2^1A_g and 1^1B_{1g} states of the neutral polyacenes. The obtained value is also in agreement with the previously mentioned two-photon experiments on naphthalene, in which a *gerade* state has been located around 5.5 eV [63–65]. Going to larger polyacenes, the accuracy of ADC(2)-s and EOM-CCSD degrades owing to the increasing importance of doubly excited configurations in the description of the wavefunction of the 2^1A_g state with growing number of fused benzene rings. Remarkably, the vertical excitation energy of pentacene drops by 3 eV going from ADC(2)-s to ADC(2)-x from 4.53 to 1.57 eV. However, also the ADC(2)-x and DFT/MRCI values deviate by 1 eV for pentacene and hexacene, the ADC(2)-x values being lower. Taking the typical 0.5 eV underestimation of the closed-shell ADC(2)-x approach into account [34, 37, 41], still 0.5 eV remain to be explained. The different ground state geometries, employed in the ADC(2)-x and DFT/MRCI calculations can be excluded as origin of these deviations. Recalculation of the excitation energies of anthracene at the ADC(2)-x level using also the DFT/B3LYP/TZVP optimized molecular geometry revealed only negligible changes of less than 0.1 eV in the vertical excitation energies. It remains to be clarified whether the observed discrepancies between DFT/MRCI and ADC(2)-x stem from increasing multi-reference character of the ground states of the polyacenes with size which is most likely not captured by the MP2 method underlying the ADC(2) approach as described in Section 2.

The second lowest excited state with *gerade* symmetry of naphthalene is the 1^1B_{1g} state at the levels of ADC(2)-s, ADC(2)-x and EOM-CCSD with excitation energies of 6.54, 5.26 and 6.85 eV, respectively. At DFT/MRCI level, as mentioned above, this state is the lowest *gerade* state of naphthalene exhibiting a vertical excitation energy of 5.63 eV. However, already for anthracene 1^1B_{1g} is the second lowest *gerade* state also at DFT/MRCI level. As for the 2^1A_g state, the vertical excitation energy drops by remarkable 1.3 eV from ADC(2)-s to ADC(2)-x underlining the importance of double excitations in the description of its wavefunction. In fact, the 1^1B_{1g} state has large contributions from singly excited determinants

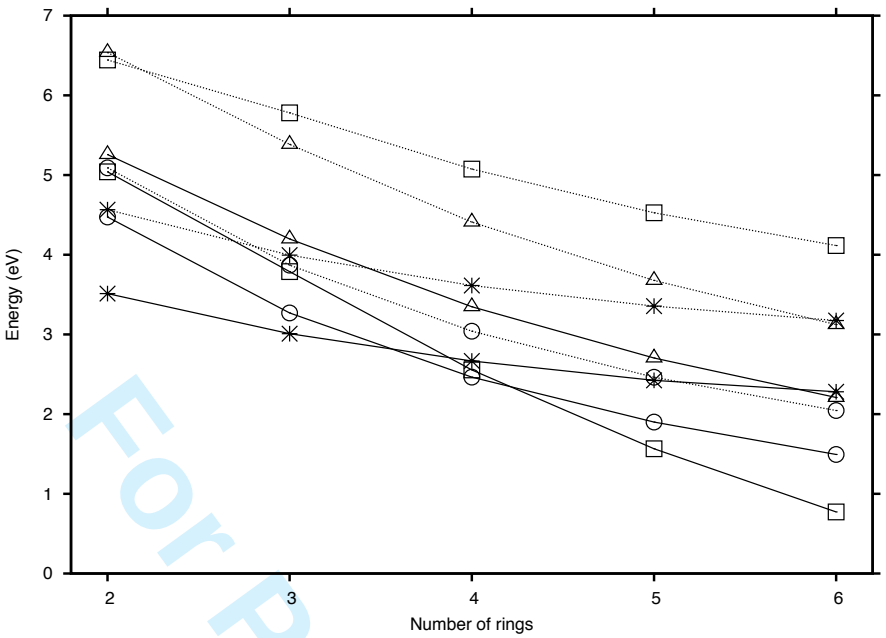

Figure 2. Excitation energies of the four lowest excited states of the neutral linear polyacenes depending on the number of fused benzene rings, calculated at the ADC(2)-s (dotted lines) and ADC(2)-x (full lines) levels using the 6-31G* basis set. A_g states are given as squares (□), B_{1g} as triangles (△), B_{2u} as circles (⊙) and B_{3u} as stars (⋇).

HOMO-2→LUMO and HOMO→LUMO+2, but with increasing size of the polyacene contributions from double excitations become more prominent. In general, the deviation between the DFT/MRCI and ADC(2)-x values is only 0.4 eV at most for all polyacenes, which is the typical underestimation of the ADC(2)-x scheme.

For large molecules, it is often very difficult or even impossible to apply multi-reference methods to take doubly excited configurations properly into account. Thus it is very important to provide a diagnostic for the detection of states with substantial double excitation character. Comparison of the results of *strict* and *extended* ADC(2) calculations offers this opportunity, since the latter significantly improves the description of states with double excitation character lowering their excitation energies relative to typical single excitations. Thereby, the relevance of doubly excited configurations in the description of low-lying excited states is revealed. This has already been demonstrated for polyenes [41–43], but can also be nicely seen in Figure 2, in which the excitation energies of the four lowest excited states 1^1B_{3u}, 1^1B_{2u}, 2^1A_g and 1^1B_{1g} obtained at ADC(2)-s and -x level are plotted against the number of fused benzene rings. While the excitation energies of these states in general decrease from ADC(2)-s to ADC(2)-x by about 1 eV shifting the curves parallel downwards, the exception is the 2^1A_g state. At ADC(2)-x level the curve is much steeper than at the ADC(2)-s level owing to the pronounced double excitation character of this state in the larger polyacenes. While the ADC(2)-s calculations yield the 2^1A_g state for all polyacenes larger than naphthalene as fourth lowest excited state, it drops drastically in energy when going to the *extended* scheme. Indeed, the ADC(2)-x calculations predict this state even to become the lowest excited state of pentacene and the larger polyacenes. Nevertheless, since the excitation energy of the A_g state is underestimated, the actually crossing point of

the 2^1A_g and 1^1B_{2u} most likely occurs later at hexacene, as has been predicted by the DFT/MRCI calculations. In summary, the comparison of ADC(2)-s and ADC(2)-x calculations is generally very helpful to identify low-lying excited states with significant double excitation character in unknown molecules for which expensive multi-reference methods are no longer feasible.

5. Excited State Properties of Polyacene Radical Cations

The radical cations of the linearly fused polyacenes exhibit a doublet open-shell electronic ground state, in which the positive charge is delocalized over the entire carbon backbone of the D_{2h} symmetric molecules. The irreducible representation of the electronic ground state changes depending on the number of fused rings. PACs with an even number of rings exhibit a ^2A_u ground state, while it is $^2B_{3g}$ for those with an odd number. However, the nature of the involved molecular orbitals stays the same for all polyacene radical cations and the frontier orbitals are displayed for naphthalene, anthracene and tetracene in Figure 3. For the classification of the molecular orbitals, we will use the following nomenclature. We will distinguish between highest doubly occupied molecular orbitals (HOMO) and lowest unoccupied molecular orbitals (LUMO), and one singly occupied molecular orbital (SOMO), since the appearance of the individually optimized α- and β-MOs in the unrestricted UHF reference determinant are practically identical. This is also noticed by the small spin contamination of the ground state UHF reference determinants, which is only 0.09 ($\langle\hat{S}^2\rangle = 0.84$)for the naphthalene radical cation and increases up to 0.29 ($\langle\hat{S}^2\rangle = 1.04$) for the radical cation of hexacene. The electron occupying the SOMO is assumed to exhibit α spin.

According to the change of the irreducible representation of the electronic ground state of the polyacene radical cations with odd or even number of fused rings, also the excited states change their symmetry classification. For example, the D_1 state of the naphthalene radical cation is a $^2B_{1u}$ state, while the corresponding one of anthracene has $^2B_{2g}$ symmetry, although the nature of these states is the same for both. The symmetry of the electronic transition, however, from the ground state into the excited state is given by the direct product of the state symmetries and is for both D_1 states of the radical cations of naphthalene and anthracene the same, i.e. B_{1g}. Therefore, the excited states of the PAC radical cations are going to be classified by their transition symmetry rather than the state symmetry. Note that for closed-shell molecules both are necessarily the same, since the ground state is always totally symmetric.

Removal of a β-electron out of the highest occupied molecular orbital of the neutral polyacenes creates a vacancy in the SOMO of the radical cations, which can be easily filled by excitation of a β-electron out of a lower lying doubly occupied orbital. Typically, these excited states exhibit very small excitation energies, sometimes even in the near IR region [81–83]. Not surprisingly, the D_1 state of naphthalene corresponds in fact to such a state, which can be best represented as an excitation of an β-electron out of the HOMO into the SOMO with a transition symmetry of B_{1g} (Table 2, Figure 3). Due to its symmetry, this transition is optically one-photon forbidden. At the theoretical levels of UADC(2)-s, UADC(2)-x and UB3LYP this state exhibits vertical excitation energies for the naphthalene radical cation of as small as 1.43, 0.62 and 1.25 eV, respectively. Unfortunately, no experimental value is available for comparison. Going to larger polyacenes, the orbital ordering is slightly changed and for anthracene and tetracene the former HOMO is now the HOMO-1, which for pentacene and hexacene becomes even the

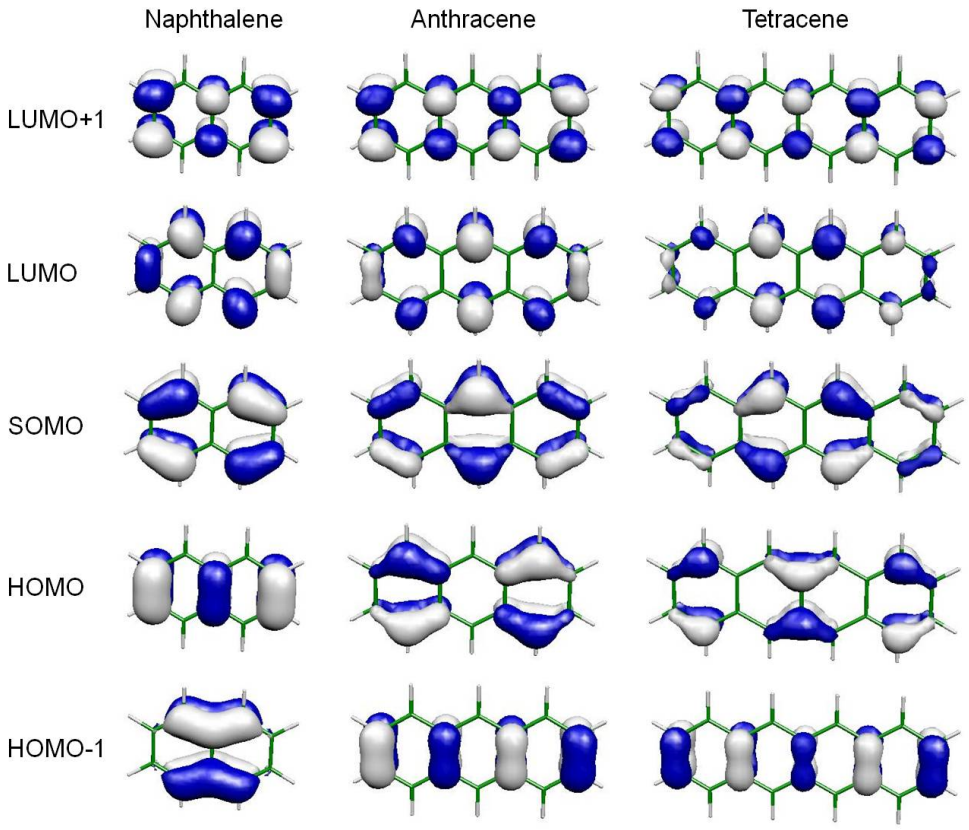

Figure 3. Frontier molecular orbitals of naphthalene, anthracene and tetracene.

HOMO-2 (Figure 3). Along with this trend, the amplitude of the β-transition out of these orbitals into the SOMO decreases from 0.89 for naphthalene to 0.50 in hexacene. Most strikingly however, the excitation energy of the B_{1g} transition *increases* from naphthalene to hexacene to values of 2.70, 1.62 and 2.15 eV at the ADC(2)-s, ADC(2)-x and UB3LYP levels, respectively. This contradicts the typical particle-in-a-box model for excited states of molecules with extended π-systems, which predicts that the excitation energies become smaller with increasing system size. This state represents an interesting exception since the excitation energies of all other states of the investigated polyacenes do indeed drop with increasing molecular size as we will see later (Figure 4).

To understand why the B_{1g} transition does behave so differently from all the other electronically excited states, one can inspect the molecular orbitals and their energies with increasing polyacene size. In figure 5, the orbital energies of the frontier orbitals are displayed. First of all, comparison of the energies of the α and β orbitals reveals that the β orbital energies are only slightly smaller than the corresponding α energies due to the missing energetically favorable exchange interactions in the β space. Only the SOMO, which is occupied by an α electron and vacant in the β orbital space, is shifted to substantially higher energies than the corresponding α, since in the former it represents the energy of an additional electron. In the case of the B_{1g} transition, an electron is excited from the βHOMO into the βSOMO in naphthaline, from βHOMO-1 to the βSOMO in anthracene and tetracene, and from βHOMO-2 to the βSOMO in the longer polyacenes, respectively. Surprisingly, the gap between these orbitals does not decrease with growing molecular size, but instead increases slightly (Figure 5). In principle, this effect can largely be ascribed to the remarkably small increase of the orbital energy of the

Table 2. Computed vertical excitation energies (eV) and oscillator strengths (in parenthesis) of the four lowest excited states of the radical cations of naphthalene (2) to hexacene (6) at UADC(2)-s, UADC(2)-x and UTDDFT/B3LYP of theory compared with literature data at TDDFT level and experimental values.

n	UADC(2)-s	UADC(2)-x	UB3LYP	UB3LYP[a]	Expt.
$1B_{1g}$					
2	1.43 (0.000)	0.62 (0.000)	1.25		
3	1.80 (0.000)	0.90 (0.000)	1.54		
4	2.16 (0.000)	1.26 (0.000)	1.83		
5	2.43 (0.000)	1.51 (0.000)	1.92		
6	2.70 (0.000)	1.62 (0.000)	2.15		
$1B_{3u}$					
2	2.46 (0.084)	1.75 (0.058)	2.52	2.14	1.84[b,d], 1.85[c]
3	2.01 (0.147)	1.19 (0.085)	1.95	1.93	1.73[e], 1.71[f], 1.75[g]
4	1.78 (0.221)	0.99 (0.121)	1.72	1.70	1.43[f,h,i]
5	1.58 (0.301)	0.78 (0.148)	1.52	1.50	1.31[k]
6	1.40 (0.385)		1.35	1.34	1.14[l]
$1B_{2u}$					
2	3.68 (0.013)	2.74 (0.012)	3.43	2.98	2.72[b,c],2.69[d]
3	2.61 (0.014)	1.79 (0.008)	2.38	2.32	2.02[e]
4	1.99 (0.023)	1.23 (0.013)	1.75	1.70	1.65[f],1.66[h,i]
5	1.53 (0.023)	0.79 (0.011)	1.28	1.25	1.27[k]
6	1.18 (0.021)	0.46 (0.007)	0.94	0.90	0.80[l]
$2A_g$					
2					
3	3.16 (0.000)	2.28 (0.000)	3.01		
4	3.11 (0.000)	2.21 (0.000)	2.77		
5	2.85 (0.000)	1.98 (0.000)	2.50		
6	2.60 (0.000)		2.24		

[a] taken from Ref. [70], who used the 6-31+G* for geometry optimization and the excited state calculations.

[b] taken from Ref. [71]

[c] taken from Ref. [72]

[d] taken from Ref. [73]

[e] taken from Ref. [74]

[f] taken from Ref. [75]

[g] taken from Ref. [76]

[h] taken from Ref. [77]

[i] taken from Ref. [78]

[k] taken from Ref. [79]

[l] taken from Ref. [80]

corresponding βHOMO with increasing size of the polyacenes, which results in an essentially flat curve in Figure 5 and an increasing HOMO-SOMO gap for this electronic transition. The corresponding HOMO (naphthalene), HOMO-1 (anthracene and tetracene) or HOMO-2 (pentacene and hexacene) exhibits a characteristic non-bonding ladder-type shape (Figure 3).

Let us now return to the description of the other low-lying electronic transitions of the linear polyacene radical cations. The second excited D_2 state of the naphthalene radical cation corresponds to a $^2B_{3u}$ transition. At the theoretical levels of ADC(2)-s, ADC(2)-x and UB3LYP, it exhibits vertical excitation energies of 2.46,

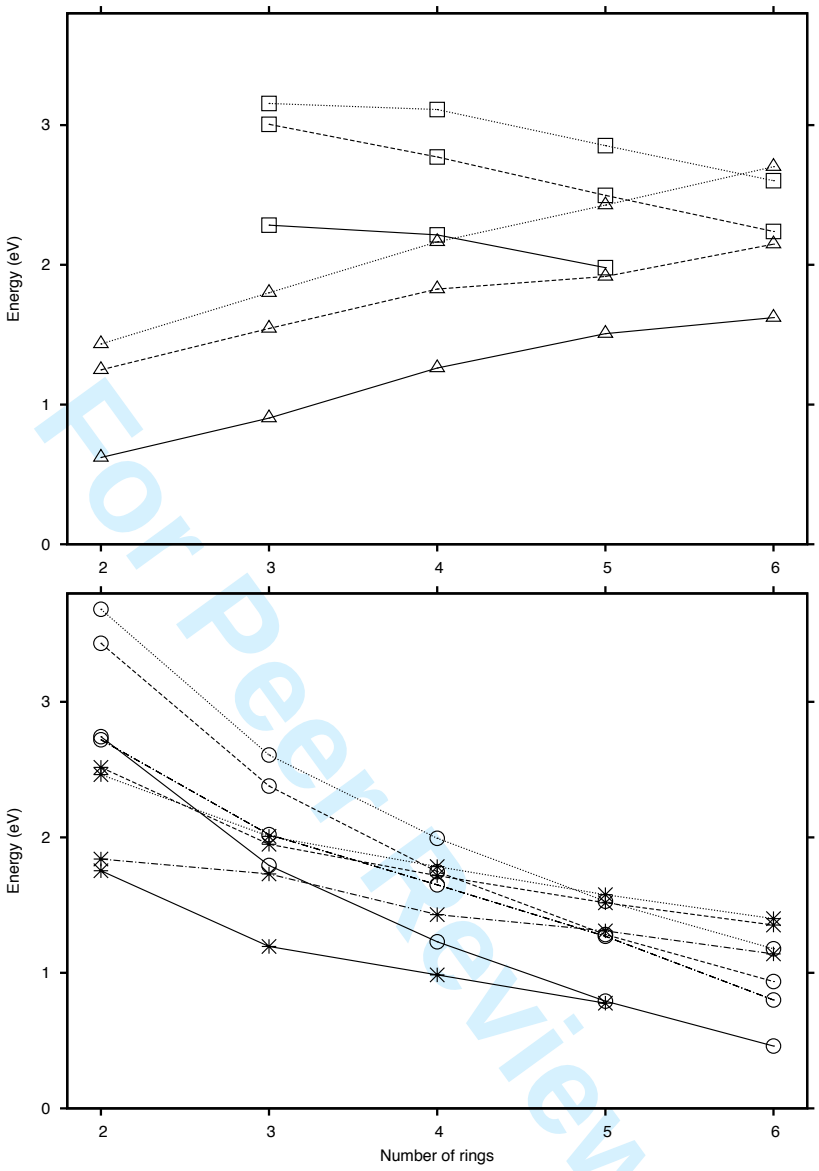

Figure 4. Comparison of the A_g (□) and B_{1g} (△) states (top) and of the B_{2u} (⊙) and B_{3u} (⋇) states (bottom) of the polyacene radical cations depending on the number of fused benzene rings at the theoretical levels of UADC(2)-s (dotted line) and UADC(2)-x (full line) with UB3LYP (dashed line) and experimental values (·—) [71, 74, 75, 79, 80].

1.75 and 2.52 eV. Using a diffuse basis set, this transition has been calculated previously using TDDFT/B3LYP to possess an excitation energy of 2.14 eV [70]. The experimental value is given as 1.84 eV [71–73]. Going to the larger polyacene radical cations, tetracene for example, the vertical excitation energies amount to 1.78, 0.99 and 1.72 eV, at the theoretical levels of ADC(2)-s, ADC(2)-x and UB3LYP, respectively. Compared to the known experimental value of 1.43 eV, one recognizes the typical overestimation of the excitation energy by ADC(2)-s and the typical underestimation by ADC(2)-x. This trend is observed also for the other excited states of the investigated polyacene radical cations. In the one-particle picture, the B_{3u} transition of the naphthalene radical cation is best described as a transition of

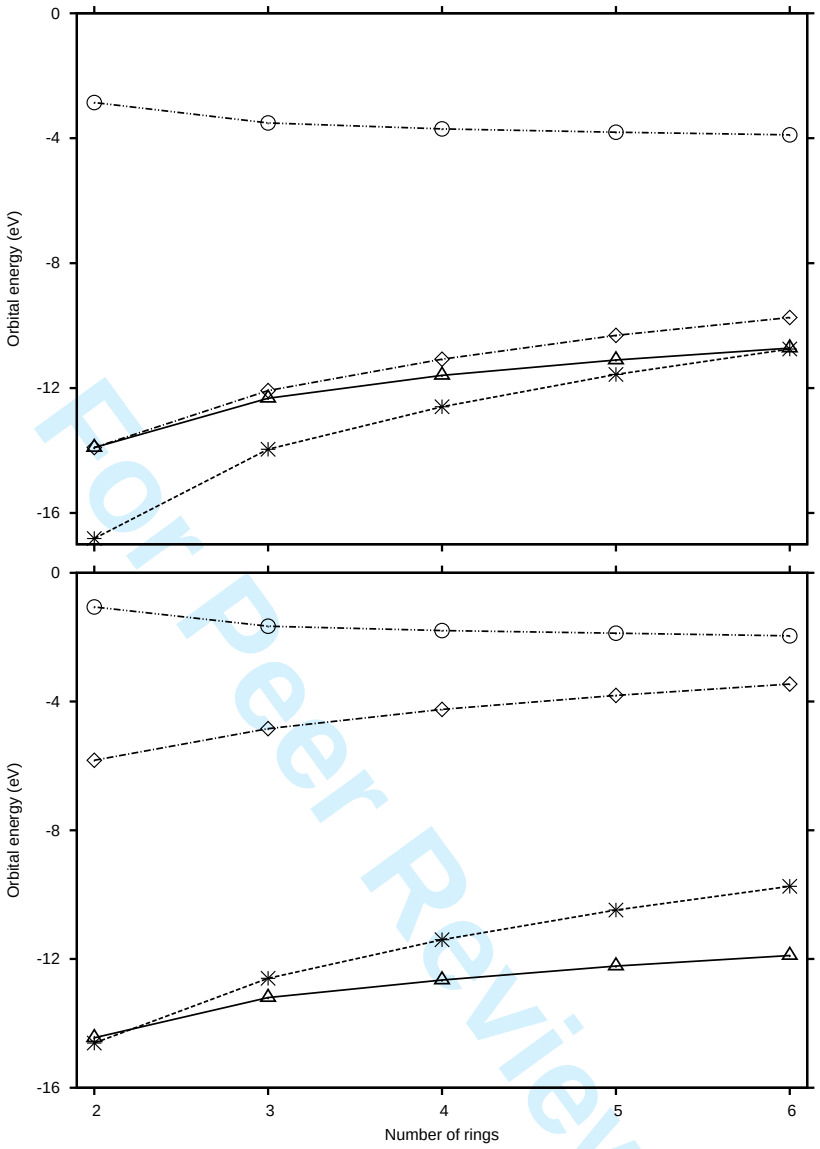

Figure 5. Orbital energies of the alpha (top) and beta (bottom) orbitals of the polyacenes as a function of the number of fused benzene rings. (HOMO, full line, △; HOMO-1, −−, ⁎; SOMO, ·−, ◊; LUMO, · · −, ⊙).

a β electron from the HOMO-1 into the SOMO. For the larger polyacene cations the HOMO and HOMO-1 orbitals change and then the B_{3u} transition becomes the HOMO to SOMO excitation (Figure 3). However, the weight of the corresponding determinant in the wavefunctions is almost constant for all polyacene radical cations with 0.87 from naphthalene to 0.82 for hexacene. Since the excitation energy of the B_{3u} transition decreases with increasing system size, it becomes the lowest excited state for tetracene at ADC(2) level, in agreement with the experimental data [75, 77, 78]. Since the B_{3u} transition is *ungerade*, it is one-photon allowed and thus exhibits substantial oscillator strength increasing from naphthalene with values of 0.084 and 0.058 at the theoretical levels of ADC(2)-s and ADC(2)-x, respectively, to 0.301 and 0.148 for pentacene, for example. This transition can be expected to dominate the absorption spectra of the polyacene radical cations in

the low-energy region.

The third lowest excited D_3 state of the naphthalene radical cation corresponds to an one-photon allowed B_{2u} transition exhibiting a vertical excitation energy of 3.68, 2.74 and 3.43 eV at the theoretical levels of ADC(2)-s, ADC(2)-x and UB3LYP, respectively. The experimental excitation energy has been found to be about 2.7 eV [71–73] for the B_{2u} transition of the naphthalene radical cation, which is in good agreement with the ADC(2)-x value. For the longer polyacene radical cations, however, ADC(2)-x underestimates the experimental values by about 0.2-0.4 eV (Table 2). Going to larger polyacene radical cations, the B_{2u} transition crosses the B_{3u} transition and also the B_{1g} transition and eventually becomes the lowest one for pentacene (Table 2, Figure 4). In the molecular orbital picture, the B_{2u} electronic transition is best described as a linear combination of two determinants, one corresponding to an excitation of an α electron from the SOMO to the LUMO (Figure 3) and one corresponding to a β-electron excitation out of the HOMO-2 into the SOMO. While the latter dominates the transition for the smaller polyacenes, the first dominates for the longer ones exhibiting transition amplitudes of about 0.8 from tetracene on. The oscillator strength of the $1B_{2u}$ transition is overall rather small at the ADC levels (Table 2).

A *gerade* A_g transition is the fourth lowest excited D_4 state of the radical cations of anthracene to pentacene, and the third lowest one of the hexacene radical cation, since it crosses the B_{1g} transition. For the naphthalene radical cation an analoguous excited state does not exist. In the one-particle picture, the A_g transition is best described as an excitation of a β-electron from the HOMO-2 to the SOMO in anthracene and tetracene or, since HOMO-2 and HOMO-1 change when going to pentacene and hexacene, from the HOMO-2 into the SOMO in the latter two longer polyacenes. The weight of the corresponding determinants in the excited state wavefunctions of the D_4 state, range between 0.78 and 0.85 for all polyacene radical cations. Due to its symmetry, the A_g transition is strictly one-photon forbidden, and cannot directly be observed in corresponding experimental spectra. At the level of ADC(2)-s the A_g transition exhibits excitation energies of 3.15, 3.11, 2.85 and 2.6 eV from anthracene up to hexacene, i.e. the vertical excitation energies decrease only very slowly with increasing polyacene size (Figure 4). Going to the ADC(2)-x level, the excitation energies drop consistently by about 0.9 eV to 2.28, 2.21 and 1.98 eV for anthracene, tetracene and pentacene, respectively. Since this state does not exhibit substantial contributions of doubly excited configurations, also unrestricted TDDFT can describe this state reasonably well. The excitation energies are found to lie between the ones given by ADC(2)-s and ADC(2)-x and exhibit values of 3.01, 2.77, 2.50 and 2.24 eV for the polyacenes from anthracene to hexacene, respectively.

Let us briefly comment on the performance of the UADC schemes and UTDDFT for the vertical excitation energies of the polyacene radical cations. It has been observed previously that ADC(2)-s tends to overestimate excitation energies by 0.3-0.5 eV, while ADC(2)-x usually underestimates them by about 0.3 eV [42]. This is also observed here for the electronic transitions for which experimental data are available for comparison, i. e. B_{2u} and B_{3u}: ADC(2)-s yields too large values by about 0.3 to 0.7 eV, while ADC(2)-x gives too small values. Unrestricted TDDFT employing the B3LYP xc-functional and the 6-31G* basis set again overestimates the excitation energies by about by 0.2 to 0.3 eV and gives the best agreement with the available experimental data. However, this is true only for the one-photon allowed *ungerade* B_{2u} and B_{3u} transitions, for which doubly excited configurations do not play an important role. The accuracy of the *gerade* transitions B_{1g} and A_g is difficult to estimate, since neither experimental nor theoretical benchmark data

is available. Anyways, since the decrease in excitation energies is practically the same for all states when going from ADC(2)-s to ADC(2)-x, one can expect the schemes to exhibit approximately the same accuracy for the four states investigated in detail here. Of course, this will be different when more energetically higher lying states are considered, where doubly excited states become more important. Then the quality of ADC(2)-s and TDDFT will degrade as has been observed for the famous $2A_g$ state of linear polyenes [41].

6. Brief Summary

The energetically low-lying excited electronic states of linearly fused polyacenes and their radical cations have been investigated using the algebraic diagrammatic construction (ADC) scheme of second order (ADC(2)). The neutral polyacenes generally pose a challenge to electronic structure theory due to an increasing multi-reference character of the ground state with increasing molecular size and the importance of doubly excited configurations for their excited states with *gerade* spatial symmetry. In addition, the availability of reliable multi-reference data, makes the polyacenes an ideal test set to challenge the accuracy and applicability of single-reference ADC(2) for such problematic cases. Our calculations have shown that strict ADC(2) (ADC(2)-s) can reproduce the trends of the singly excited states B_{2u} and B_{3u} with essentially the same accuracy as CC2, and, analogously, can not describe the *gerade* states A_g and B_{1g} exhibiting mostly double excitation character. The description of these doubly excited states is largely improved when extended ADC(2) (ADC(2)-x) is used, and the excitation energies are observed to drop substantially from the ADC(2)-s to the ADC(2)-x level. However, for the longer polyenes an atypically large underestimation of the excitation energies at ADC(2)-x level is observed, which is attributed to the pronounced multi-reference character of the neutral polyacenes. Nevertheless, a combined application of both ADC(2)-s and ADC(2)-x is extremely useful for the identification of the importance of doubly excited configuration for a correct description of the excited state spectrum of unknown molecules, for which expensive multi-reference approaches are not feasible.

The theoretical investigation of the radical cations of the polyacenes employing unrestricted ADC (UADC) revealed that neither doubly excited states nor a multi-reference treatment are critically important for the theoretical description of the low-lying excited states. While UADC(2)-s tends to overestimate the excitation energies by about 0.3-0.5 eV, UADC(2)-x yields too low excitation energies by essentially the same amount. Also UTDDFT is capable of describing the low-lying excited states of the polyacenes reasonably well.

As is generally expected, the vertical excitation energies of the neutral polyacenes have been found to decrease with increasing molecular size. This is also the case for most of the excited states of the radical cations, however, our computations identified one B_{1g} transition, whose excitation energy increases with increasing size of the polyacenes. This excited state can be described as an excitation of a β electron out of the lowest doubly occupied molecular orbital (HOMO) into the singly occupied one (SOMO). Such states do not exist in neutral closed-shell systems, and are here made possible by ionization, i.e. removal of an electron out of the HOMO and thereby creating a vacancy into which another electron can now be excited. The fact that the excitation energy of this transition increases with increasing polyacene size is explained with the increasing energy gap between the orbital out of which is excited and the SOMO.

Acknowledgements

AD acknowledges financial support from the Deutsche Forschungsgemeinschaft as a Heisenberg professor. Computation time has been generously provided by the Center of Scientific Computation of the University of Frankfurt.

References

[1] S. Grimme, Rev. Comp. Chem. **20**, 153 (2004).
[2] A. Dreuw, Chem. Phys. Chem. **7**, 2259 (2006).
[3] E. Runge and E.K.U. Gross, Phys. Rev. Lett. **52**, 997 (1984).
[4] M.E. Casida, in , edited by D. P. Chong (World Scientific, Singapore, 1995), pp. 155–192.
[5] A. Dreuw and M. Head-Gordon, Chem. Rev. **105**, 4009 (2005).
[6] D. Hegarthy and M.A. Robb, Mol. Phys. **38**, 1795 (1979).
[7] R.H.E. Eade and M.A. Robb, unknownChem. Phys. Lett. **83**, 362 (1981).
[8] H. Nakatsuji and K. Hirao, J. Chem. Phys. **68**, 2053 (1978).
[9] O. Christiansen, H. Koch and P. Jørgensen, J. Chem. Phys. **103**, 7429 (1995).
[10] O. Christiansen, H. Koch and P. Jørgensen, Chem. Phys. Lett. **243**, 409 (1995).
[11] H. Koch, O. Christiansen, P. Jørgensen, T. Helgaker and A.S. de Meras, J. Chem. Phys. **106**, 1808 (1997).
[12] C. Haettig and F. Weigend, J. Chem. Phys. **113**, 5154 (2000).
[13] A.L. Sobolewski and W. Domcke, Eur. Phys. J. D **20**, 369 (2002).
[14] A.L. Sobolewski, W. Domcke, C. Dedonder-Lardeux and C. Jouvet, Phys. Chem. Chem. Phys. **4**, 1093 (2002).
[15] A.L. Sobolewski and W. Domcke, Phys. Chem. Chem. Phys. **6**, 2763 (2004).
[16] S. Grimme and M. Waletzke, J. Chem. Phys. **111**, 5645 (1999).
[17] K.A. Seefeld, C. Plützer, D. Löwenich, T. Häber, L. R, K. Kleinermanns, J. Tatchen and C.M. Marian, Phys. Chem. Chem. Phys. **7**, 3021 (2005).
[18] C.M. Marian, D. Nolting and R. Weinkauf, Phys. Chem. Chem. Phys. **7**, 3306 (2005).
[19] A. Damjanovic, H.M. Vaswani, P. Fromme and G.R. Fleming, J. Phys. Chem. B **106**, 10251 (2002).
[20] M. Dierksen and S. Grimme, J. Chem. Phys. **120**, 3544 (2004).
[21] M. Dierksen and S. Grimme, J. Phys. Chem. A **108**, 10225 (2004).
[22] M. Garavelli, p. Celani, F. Bernardi, M.A. Robb and M. Olivucci, J. Am. Chem. Soc. **119**, 6891 (1997).
[23] A. Migani, M.A. Robb and M. Olivucci, J. Am. Chem. Soc. **125**, 2804 (2003).
[24] F. Blomgren and S. Larsson, Chem. Phys. Lett. **376**, 704 (2003).
[25] K. Emrich, Nuc. Phys. **A351**, 379 (1981).
[26] H. Sekino and R.J. Bartlett, Int. J. Quant. Chem. Symp. **18**, 255 (1984).
[27] H.J. Monkhorst, Int. J. Quant. Chem. Symp. **11**, 421 (1977).
[28] D. Mukherjee and P. Mukherjee, Chem. Phys. **39**, 325 (1979).
[29] H. Koch and P. Jørgensen, J. Chem. Phys. **93**, 3333 (1990).
[30] P.E.M. Siegbahn, Chem. Phys. Lett. **109**, 417 (1984).
[31] B.O. Roos, Adv. Chem. Phys. **69**, 399 (1987).
[32] M.A. Robb and U. Niazi, Reports in Molecular Theory **1**, 23 (1990).
[33] J. Schirmer, Phys. Rev. A **26**, 2395 (1982).
[34] A.B. Trofimov and J. Schirmer, J. Phys. B **28**, 2299 (1995).
[35] A.B. Trofimov, G. Stelter and J. Schirmer, J. Chem. Phys. **111**, 9982 (1999).
[36] A.B. Trofimov, G. Stelter and J. Schirmer, J. Chem. Phys. **117**, 6402 (2002).
[37] J. Schirmer and A.B. Trofimov, J. Chem. Phys. **120**, 11449 (2004).
[38] J. Linderberg and Y. Öhrn, *Propagators in Quantum Chemistry* (, , 2004).
[39] L.S. Cederbaum, in *Encyclopedia of Computational Chemistry*, edited by P. v. R. Schleyer, N. L. Clark, J. Gasteiger, H. F. Schaefer III. and P. R. Schreiner (Wiley, Chichester, 1998).
[40] C. Haettig, Adv. Quant. Chem. **50**, 37 (2005).
[41] J.H. Starcke, M. Wormit, J. Schirmer and A. Dreuw, Chem. Phys. **329**, 39 (2006).
[42] J.H. Starcke, M. Wormit and A. Dreuw, J. Chem. Phys. **130**, 024104 (2009).
[43] J.H. Starcke, M. Wormit and A. Dreuw, J. Chem. Phys. **131**, 144311 (2009).
[44] R.F. Curl, Nature **363**, 14 (1993).
[45] C.J. Pope, J.A. Marr and J.B. Howard, J. Chem. Phys. **97**, 11001 (1993).
[46] A.G.G.M. Tielens, *The Physics and Chemistry of the Interstellar Medium* (Cambridge University Press, Cambridge, 2005).
[47] D. Biermann and W. Schmidt, J. Am. Chem. Soc. **102**, 3163 (1986).
[48] K.N. Houk, P.S. Lee and M.J. Nendel, J. Org. Chem. **66**, 5571 (2001).
[49] V.Y. Butko, X. Chi, D.V. Lang and A.P. Ramirez, Appl. Phys. Lett. **83**, 4773 (2003).
[50] J. Lee, S.S. Kim, K. Kim, J.H. Kim and S. Im, Appl. Phys. Lett. **84**, 1701 (2004).
[51] M. Bendikov, F. Wudl and D.F. Perepichka, Chem. Rev. **104**, 4891 (2004).
[52] M. Bendikov, H.M. Duong, K. Starkey, K.N. Houk, E.A. Carter and F. Wudl, J. Am. Chem. Soc. **126**, 7416 (2004).
[53] E.S. Kadantsev, M.J. Stott and A. Rubio, J. Chem. Phys. **124**, 134901 (2006).
[54] F. Mertins and J. Schirmer, Phys. Rev. A **53**, 2140 (1996).
[55] R. Manne, Chem. Phys. Lett. **45**, 470 (1977).
[56] E. Dalgaard, Int. J. Quant. Chem. **15**, 169 (1979).
[57] J. Schirmer, Phys. Rev. A **43**, 4647 (1991).

[58] J. Schirmer and F. Mertins, Int. J. Quant. Chem. **58**, 329 (1996).
[59] F. Mertins, J. Schirmer and A. Tarantelli, Phys. Rev. A **53**, 2153 (1996).
[60] J. Schirmer and F. Mertins, Theo. Chem. Acc. **125**, 145 (2010).
[61] Y. Shao, L.F. Molnar, Y. Jung, J. Kussmann, C. Ochsenfeld, S.T. Brown, A.T.B. Gilbert, L.V. Slipchenko, S.V. Levchenko, D.P. O'Neill, R.A.D. Jr., R.C. Lochan, T. Wang, G.J.O. Beran, N.A. Besley, J.M. Herbert, C.Y. Lin, T.V. Voorhis, S.H. Chien, A. Sodt, R.P. Steele, V.A. Rassolov, P.E. Maslen, P.P. Korambath, R.D. Adamson, B. Austin, J. Baker, E.F.C. Byrd, H. Dachsel, R.J. Doerksen, A. Dreuw, B.D. Dunietz, A.D. Dutoi, T.R. Furlani, S.R. Gwaltney, A. Heyden, S. Hirata, C.P. Hsu, G. Kedziora, R.Z. Khalliulin, P. Klunzinger, A.M. Lee, M.S. Lee, W. Liang, I. Lotan, N. Nair, B. Peters, E.I. Proynov, P.A. Pieniazek, Y.M. Rhee, J. Ritchie, E. Rosta, C.D. Sherrill, A.C. Simmonett, J.E. Subotnik, H.L.W. III, W. Zhang, A.T. Bell and A.K. Chakraborty, Phys. Chem. Chem. Phys. **8**, 3172–3191 (2006).
[62] A.I. Krylov, Ann. Rev. Phys. Chem. **59**, 433 (2008).
[63] A. Bergmann and J. Jortner, Chem. Phys. Lett. **26**, 323 (1974).
[64] N. Mikami and M. Ito, Chem. Phys. Lett. **31**, 472 (1975).
[65] R.T. Lynch, Jr. and H. Lotem, J. Chem. Phys. **66**, 1905 (1977).
[66] P. Tavan and K. Schulten, J. Chem Phys. **70**, 5415 (1979).
[67] C.M. Marian and N. Gilka, J. Chem. Theo. Comp. **4**, 1501 (2008).
[68] S. Grimme and M. Parac, Chem.Phys.Chem. **4**, 292 (2003).
[69] M. Parac and S. Grimme, Chem. Phys. **292**, 11 (2003).
[70] G. Malloci, G. Mulas, G. Cappellini and C. Joblin, Chem .Phys. **340**, 43 (2007).
[71] F. Salama and L.J. Allamandola, J. Chem. Phys. **94**, 6964 (1991).
[72] T. Pino, N. Boudin and P. Brechignac, J. Chem. Phys. **111**, 7337 (1999).
[73] B.J. Kelsall and L. Andrews, J. Chem. Phys. **76**, 5005 (1982).
[74] J. Szczepanski, M. Vala, D. Talbi, O. Parisel and Y. Ellinger, J. Chem. Phys. **98**, 4494 (1993).
[75] T. Shida and S. Iwata, J. Am. Chem. Soc. **95**, 3473 (1973).
[76] O. Sukhorukov, A. Staicy, E. Diegel, G. Rouille, T. Henning and F. Huisken, Chem. Phys. Lett. **386**, 259 (2004).
[77] L. Andrews, R.S. Friedmann and B.J. Kelsall, J. Phys. Chem. **89**, 4016 (1985).
[78] J. Szczepanski, J. Drawdy, C. Walburg and M. Vala, Chem. Phys. Lett. **245**, 539 (1995).
[79] T.M. Halasinski, D.M. Hudgins, F. Salama, L.J. Allamanola and T. Bally, J. Phys. Chem. A **104**, 7484 (2000).
[80] R. Mondal, C. Tönshoff, D. Khon, D.C. Neckers and H.F. Bettinger, J. am. Chem. Soc. **131**, 14281 (2009).
[81] T.M. Halasinski, J.L. Weisman, R. Ruiterkamp, T.J. Lee, F. Salama and M. Head-Gordon, J. Phys. Chem. A **107**, 3660 (2003).
[82] J.L. Weisman, T. J.Lee, F. Salama and M. Head-Gordon, Astrophys. J. **587**, 256 (2003).
[83] J.L. Weisman, A. Mattioda, T. J.Lee, D. Hudgins, L.J. Allamandola, C.W. Bauschlicher and M. Head-Gordon, Phys. Chem. Chem. Phys. **7**, 109 (2005).